Article

Cell Metabolism

The Chromatin Remodeling Complex Chd4/NuRD Controls Striated Muscle Identity and Metabolic Homeostasis

Graphical Abstract

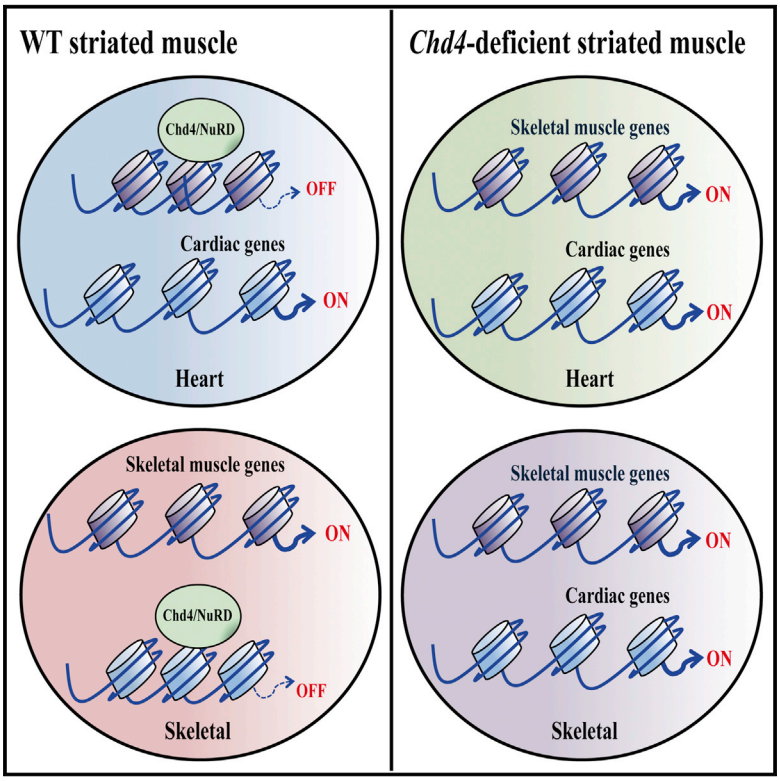

Highlights

- Chd4/NuRD complex regulates the lineage-specific gene expression of striated muscles
- Loss of Chd4 in skeletal muscle causes inappropriate expression of cardiac genes
- Chd4 deficiency leads to cardiac and skeletal myopathies and sudden death
- Chd4/NuRD regulates mitochondrial homeostasis in striated muscles

Authors

Pablo Gómez-del Arco,
Eusebio Perdiguero,
Paula Sofia Yunes-Leites, ...,
Esteban Ballestar,
Pura Muñoz-Cánoves,
Juan Miguel Redondo

Correspondence

pablo.gomez@uam.es (P.G.A.),
jmredondo@cnic.es (J.M.R.)

In Brief

Despite similar organization, heart and skeletal muscles use lineage-specific sarcomeric proteins for contraction. Gómez-del Arco et al. show that the chromatin-remodeling complex Chd4/NuRD preserves the identity of each striated muscle by epigenetic repression of the alternate lineage gene expression program. Furthermore, this complex also maintains metabolic homeostasis in both striated tissues.

Gómez-del Arco et al., 2016, Cell Metabolism *23*, 881–892
May 10, 2016
http://dx.doi.org/10.1016/j.cmet.2016.04.008

Cell Metabolism
Article

The Chromatin Remodeling Complex Chd4/NuRD Controls Striated Muscle Identity and Metabolic Homeostasis

Pablo Gómez-del Arco,[1,2,*] Eusebio Perdiguero,[3] Paula Sofia Yunes-Leites,[1] Rebeca Acín-Pérez,[4] Miriam Zeini,[1] Antonio Garcia-Gomez,[5] Krishnamoorthy Sreenivasan,[6] Miguel Jiménez-Alcázar,[1] Jessica Segalés,[3] Dolores López-Maderuelo,[1] Beatriz Ornés,[1] Luis Jesús Jiménez-Borreguero,[7,8] Gaetano D'Amato,[9] David Enshell-Seijffers,[10] Bruce Morgan,[11] Katia Georgopoulos,[11] Abul B.M.M.K. Islam,[12] Thomas Braun,[6] José Luis de la Pompa,[9] Johnny Kim,[6] José A. Enriquez,[4] Esteban Ballestar,[5] Pura Muñoz-Cánoves,[3,13] and Juan Miguel Redondo[1,*]

[1]Gene Regulation in Cardiovascular Remodelling & Inflammation laboratory, Centro Nacional de Investigaciones Cardiovasculares Carlos III (CNIC), Madrid 28029, Spain
[2]Department of Molecular Biology, Universidad Autónoma de Madrid, Cantoblanco, Madrid 28049, Spain
[3]Department of Experimental & Health Sciences, University Pompeu Fabra (UPF)/CIBERNED/ICREA, Barcelona 08003, Spain
[4]Physiopathology of the Myocardium Programme, CNIC, Madrid 28029, Spain
[5]Chromatin and Disease Group, Cancer Epigenetics and Biology Programme (PEBC), Bellvitge Biomedical Research Institute (IDIBELL), 08908 L'Hospitalet de Llobregat, Barcelona 08908, Spain
[6]Department of Cardiac Development and Remodelling, Max Planck Institute for Heart and Lung Research, Bad Nauheim 61231, Germany
[7]Department of Epidemiology, Atherotrombosis and Image, CNIC, Madrid 28029, Spain
[8]Instituto de Investigación Sanitaria del Hospital Universitario de La Princesa, Madrid 28013, Spain
[9]Intercellular Signaling in Cardiovascular Development & Disease Laboratory, CNIC, Madrid 28029, Spain
[10]Faculty of Medicine in the Galilee, Bar-Ilan University, Safed 1589, Israel
[11]Cutaneous Biology Research Center, Massachusetts General Hospital, Charlestown, MA 02129, USA
[12]Department of Genetic Engineering & Biotechnology, University of Dhaka, Dhaka 1000, Bangladesh
[13]Tissue Regeneration laboratory, CNIC, Madrid 28029, Spain
*Correspondence: pablo.gomez@uam.es (P.G.A.), jmredondo@cnic.es (J.M.R.)
http://dx.doi.org/10.1016/j.cmet.2016.04.008

SUMMARY

Heart muscle maintains blood circulation, while skeletal muscle powers skeletal movement. Despite having similar myofibrilar sarcomeric structures, these striated muscles differentially express specific sarcomere components to meet their distinct contractile requirements. The mechanism responsible is still unclear. We show here that preservation of the identity of the two striated muscle types depends on epigenetic repression of the alternate lineage gene program by the chromatin remodeling complex Chd4/NuRD. Loss of Chd4 in the heart triggers aberrant expression of the skeletal muscle program, causing severe cardiomyopathy and sudden death. Conversely, genetic depletion of Chd4 in skeletal muscle causes inappropriate expression of cardiac genes and myopathy. In both striated tissues, mitochondrial function was also dependent on the Chd4/NuRD complex. We conclude that an epigenetic mechanism controls cardiac and skeletal muscle structural and metabolic identities and that loss of this regulation leads to hybrid striated muscle tissues incompatible with life.

INTRODUCTION

The myofibrilar sarcomere is a highly organized structure responsible for contraction of heart and skeletal striated muscles, requiring continuous energy supply from the mitochondria (Estrella and Naya, 2014; Fan and Evans, 2015; Wenz et al., 2008). Despite distinct embryonic origins, cardiac and skeletal striated muscles share similar contractile structures, differing in the composition of specific sarcomeric protein isoforms, which are encoded by different genes in each tissue. How differential expression of tissue-specific sarcomeric components is controlled remains largely unknown (Braun and Gautel, 2011; Buckingham and Rigby, 2014; Estrella and Naya, 2014). Potential interactions between transcription factors and epigenetic regulators may determine the distinct identities of the two striated muscle types by supporting differential gene expression (Bruneau, 2010; Chang and Bruneau, 2012; Segalés et al., 2015).

The chromatin remodeling complex NuRD (Nucleosome Remodeling and Deacetylation) plays a key role in various cellular processes, including cell-cycle progression, stem cell biology, DNA damage responses, and the maintenance of genome integrity (Hu and Wade, 2012; Kashiwagi et al., 2007; Lai and Wade, 2011; Laugesen and Helin, 2014; O'Shaughnessy-Kirwan et al., 2015; Reynolds et al., 2012; Williams et al., 2004; Zhang et al., 2012), but its function in organogenesis and postnatal organ/tissue differentiation and maintenance has only been established for the immune system (Gregory et al., 2010; Naito et al., 2007;

Williams et al., 2004; Yoshida et al., 2008; Zhang et al., 2012). The NuRD complex contains several protein components that assemble in a combinatorial manner, leading to different outcomes and cell-type-specific functions: the core NuRD subunits, chromodomain-helicase-DNA-binding proteins 3 (Chd3 or Mi-2α) and 4 (Chd4 or Mi-2β), both endowed with helicase/ATPase activity, MTA (metastasis-associated protein), and the members of the methyl-CpG-binding domain family of proteins, Mbd2 or Mbd3, which assemble into mutually exclusive Chd4/NuRD-like complexes (Le Guezennec et al., 2006). Two other NuRD components, class I histone deacetylases 1 and 2 (Hdac1 and Hdac2), also form part of other chromatin repressive complexes (Mathiyalagan et al., 2014); these components regulate striated muscle homeostasis, but it is not known if this role is dependent on the NuRD complex (Montgomery et al., 2007; Moresi et al., 2012).

In the present study, we demonstrate an essential role of Chd4/NuRD in the control of striated muscle structural and metabolic identity. We show that this chromatin remodeling complex regulates cardiomyocyte identity by silencing the skeletal muscle lineage gene program in both developing and differentiated cardiomyocytes. Conversely, cardiac genes are silenced by Chd4/NuRD in skeletal muscle. Derepression of these alternate programs by deletion of *Chd4* in mice causes lethal cardiovascular malformations in the embryo and sudden death in the adult, linked to cardiomyopathy, arrhythmias, and associated fibrosis in the heart, and severe disruption of tissue homeostasis in the skeletal muscle. Deletion of *Chd4* also leads to deregulation of mitochondrial genes in both striated muscle tissues, resulting in altered mitochondrial energetics. These findings provide insights into the transcriptional regulation of striated muscle and the establishment of cardiac and skeletal muscle identities by the chromatin remodeling complex Chd4/NuRD.

RESULTS

Chd4 Deficiency Disrupts Heart Development and Induces Cardiomyopathy in Adult Heart

To study the role of the chromatin remodeling complex Chd4/NuRD, we conditionally ablated the $Chd4^{floxed}$ allele (Williams et al., 2004) in cardiomyocytes using two different Cre deletion systems active in differentiating cardiomyocytes: the $Nkx2\text{-}5^{Cre/+}$ (Stanley et al., 2002) line and the cardiac troponin T Cre line ($Tnnt2^{Cre/+}$; Jiao et al., 2003). $Chd4^{floxed}$;$Nkx2\text{-}5^{Cre/+}$ ($Chd4^{Nkx}$);ROSA26/YFP embryos showed Cre activity in the heart and branchial arches by embryonic day 9.5 (E9.5), with no morphological differences from wild-type (WT) hearts at this stage (Figure S1A). Chd4 protein was expressed normally in epicardial or endocardial cells but not detected in mutant cardiomyocytes (Figure S1A). At E10.5, mutant embryos appeared grossly normal but had thinner ventricular compact myocardium, less intricate trabeculae, and defects in ventricular septum formation (Figure 1A). These abnormalities were more evident at E11.5, and histological analysis showed that the mutant hearts were developmentally delayed compared to WT (Figure 1B). No ventricular septum was formed in the mutants, the compact myocardium was 60% thinner, and the trabecular network was poorly developed (Figure 1B). $Chd4^{Nkx}$ embryos were alive at the expected Mendelian ratio until E12.5, but their number diminished by E13.5, and nearly all embryos were dead by E14.5 (Figure S1B). Consistent with proliferation defects described in other developing tissues (O'Shaughnessy and Hendrich, 2013), the thin compact myocardium wall in $Chd4^{Nkx}$ mutant hearts suggested impaired cardiomyocyte proliferation. Staining for Ki67 in E11.5 hearts confirmed that *Chd4* deletion reduced cardiomyocyte proliferation in the myocardium of the ventricular compact wall by 43% (Figure 1C), suggesting that this was the primary cause of the thin compact myocardium. Poor development of the compact myocardium was revealed by the reduced expression of the compact myocardium marker *Hey2* in E10.5 $Chd4^{Nkx}$ mutant hearts (Figures 1D and S1C), whereas trabecular markers *Bmp10* and *Anf* appeared to be unaffected (Figure S1D). *Mycn*, another well-established cardiomyocyte proliferation marker, appeared to be less expressed in the compact myocardium of mutant embryos (Figure S1D), although its mRNA expression in the whole heart did not show changes, possibly due to an overall compensation of expression in other heart structures (Figure S1C). Corroborating the $Chd4^{nkx}$ phenotype, the $Chd4^{floxed}$;$Tnnt2^{Cre/+}$ ($Chd4^{Tnnt2}$) embryos did not survive past E14.5 (Figure S2A), and their hearts had an underdeveloped appearance on histological analysis, with a thin compact myocardium, an underdeveloped trabeculae, and an immature ventricular septum (Figure S2B). Taken together, these data point to Chd4 as a crucial regulator of cardiomyocyte proliferation in the compact myocardium.

To study whether Chd4/NuRD also plays a role in adult heart homeostasis, we deleted *Chd4* in terminally differentiated cardiomyocytes by crossing $Chd4^{floxed}$ mice with the Corin-Cre postnatal driver line (Enshell-Seijffers et al., 2010). $Chd4^{floxed}$;$Corin^{Cre/Cre}$ ($Chd4^{corin}$) mice developed normally but died suddenly during the first 3 months of life (Figure 2A). Mutant hearts were grossly normal at 4 weeks of age (Figure 2B), but from 6 to 8 weeks onward all of the mutants analyzed showed atrial dilatation and fibrotic collagen accumulation mostly in the interventricular septum and left ventricle (Figures 2B and 2C). Cardiomyopathy is often characterized by hypertrophy, but $Chd4^{corin}$ hearts showed no sign of cardiac hypertrophy when tested by heart-to-body-weight ratio nor by cardiomyocyte cross-sectional area measurements with wheat germ agglutinin (WGA) staining (Figure 2D and data not shown). Echocardiography and electrocardiography analyses revealed defective contraction and impaired cardiac function of $Chd4^{corin}$ mice compared with controls. $Chd4^{corin}$ mice showed a significantly lower ejection fraction (Figure 2E) and cardiac arrhythmias at later disease stages (Figure 2F). In light of these results, the observed cardiac fibrosis might indicate progression of diseased $Chd4^{corin}$ hearts to heart failure. Supporting this possibility, earlier deletion of *Chd4* with the $\alpha\text{-}MHC^{Cre/+}$ line ($Chd4^{myh6}$) (Agah et al., 1997) led to postnatal death soon after weaning (Figure S2C). $Chd4^{myh6}$ mutant mice also showed earlier atrial dilatation and extensive cardiac fibrosis (Figure S2D). Together, these results indicate that the chromatin helicase Chd4 is required for the maintenance of cardiomyocyte integrity and normal cardiac function.

Chd4 Represses the Skeletal Muscle Gene Program in the Adult and Embryonic Heart

To gain insight into the molecular mechanism underlying the phenotypes observed in embryonic and adult *Chd4*-deficient

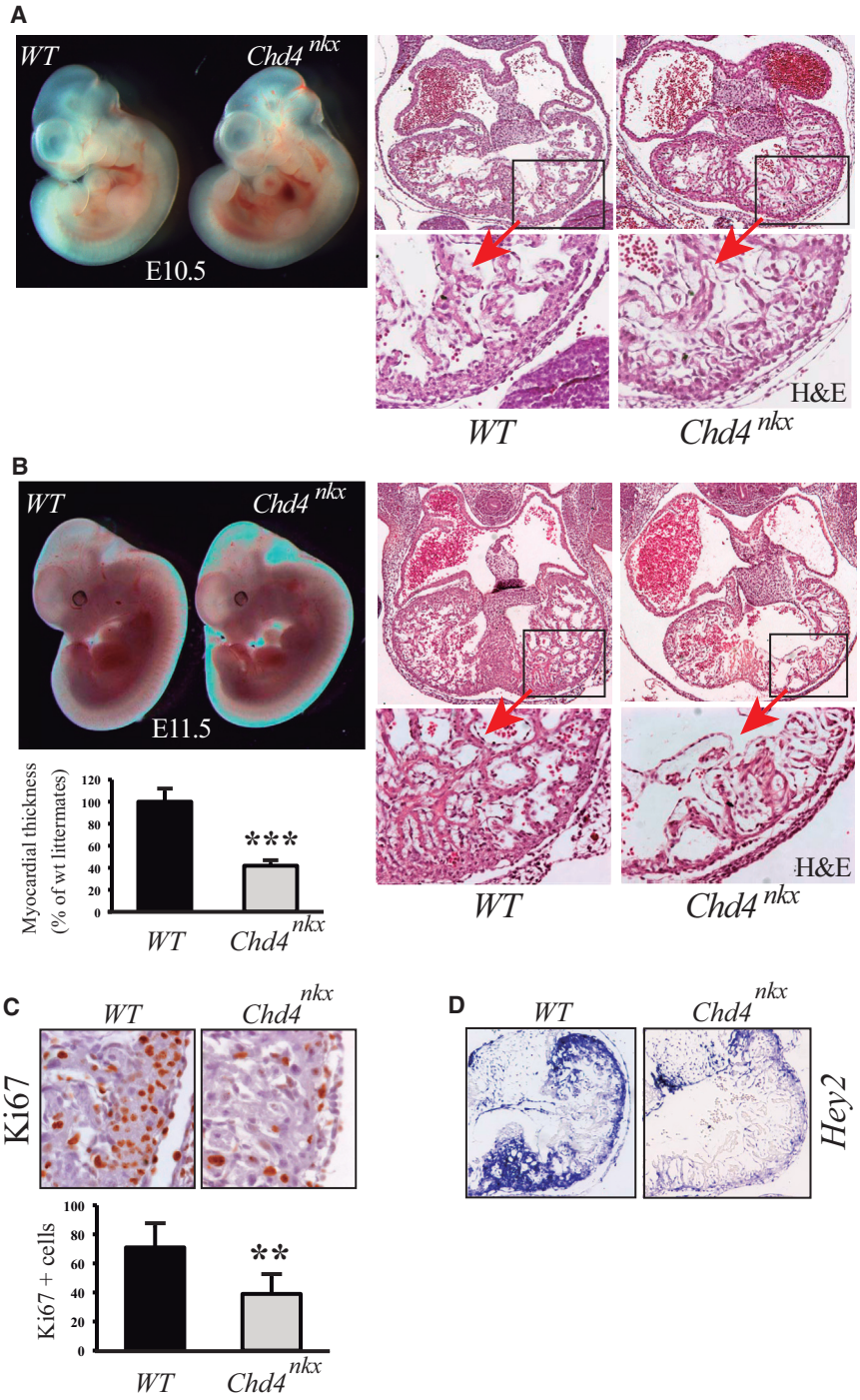

Figure 1. Chd4 Regulates Cardiomyocyte Differentiation

(A and B) Gross morphological appearance of WT and *Chd4*^{nkx} mutant E10.5 (A) and E11.5 (B) embryos (left panels). H&E staining of WT and mutant hearts (upper right panels, with insets showing magnifications of left ventricles), and corresponding ventricular compact wall thickness measurements (B) in E11.5 embryos from two independent litters (lower left panel). ***p $\leq$ 0.001 (bars express mean + SD).

(C) Ki67 immunohistochemistry (IHC) of representative E11.5 WT and *Chd4*^{nkx} embryonic hearts (top) and corresponding quantification (bottom); **p $\leq$ 0.005 (mean + SD).

(D) *Hey2* in situ hybridization (ISH) in E10.5 embryonic hearts.

mice, we performed global gene expression analysis of the whole heart by RNA-seq in *Chd4*-deficient adult mice (*Chd4*^{corin} and *Chd4*^{myh6}) and mutant E10.5 embryos (*Chd4*^{Nkx}). We first analyzed gene expression changes in mutant hearts from 4-week-old *Chd4*^{corin} and 2-week-old *Chd4*^{myh6} mice. We found 570 and 422 transcripts with a >2-fold upregulation in *Chd4*^{corin} and *Chd4*^{myh6} mice, respectively, with 240 transcripts common to both (Figure 3A and Table S1). Gene ontology (GO) functional annotation of the common upregulated transcripts (Dennis et al., 2003) identified, among other categories, significant enrichment in genes encoding sarcomeric proteins of the skeletal muscle lineage (Figure S3A). Comparison of this set of common genes with heart and skeletal muscle lineage-specific gene sets revealed that 29 skeletal muscle transcripts were upregulated in *Chd4*-deficient hearts (Figure S3B). Indeed, skeletal muscle-specific genes were the most over-represented in the upregulated transcripts in *Chd4*-deficient hearts using Tissue Specific Enrichment Analysis (TSEA) (Figures 3B and S3C). Moreover, Gene Set Enrichment Analysis (GSEA) (Asp et al., 2011) of the skeletal muscle and heart-specific gene sets revealed significant enrichment of skeletal muscle genes (Figure S3D). A similar correlation was observed when *Chd4*^{myh6} mutant hearts were analyzed (data not shown). Notably, of the downregulated genes, 84 transcripts were common to *Chd4*^{corin} and *Chd4*^{myh6} adult mutant hearts and were mainly related to mitochondrial and metabolic muscle processes, suggesting a role of Chd4 in the control of mitochondrial homeostasis during normal cardiomyocyte physiology (Figures S3E and S3F).

In the embryonic *Chd4*^{Nkx} mutant hearts, 21 genes were downregulated and 241 upregulated (>2-fold). Of the upregulated genes, 50 were also found in the upregulated gene sets in both adult mutant models (Figure S4A and Table S1). Comparison of this set of common genes with heart and skeletal muscle lineage-specific gene sets revealed that 11 skeletal muscle transcripts were commonly upregulated in all *Chd4*-deficient cardiomyocytes (Figure S4B and Table S1) and enriched in the skeletal muscle myofibril category (Figure S4C). In *Chd4*^{corin} adult hearts and *Chd4*^{nkx} E10.5 embryos, we validated the ectopic

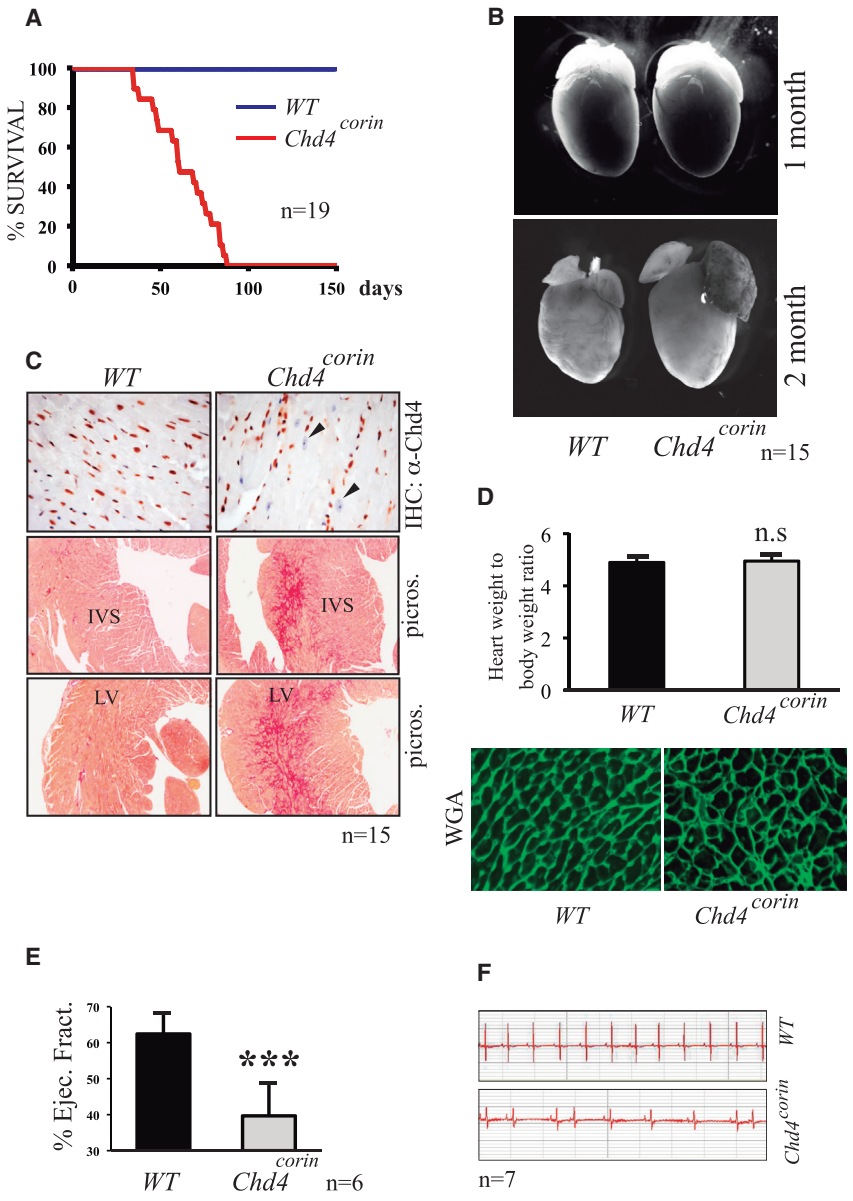

Figure 2. Chd4 Regulates Adult Heart Homeostasis

(A) Kaplan-Meier survival curve for WT and *Chd4*^{corin} mutant mice.

(B) Morphological appearance of representative (n = 15) hearts from 1-month-old (top) and 2-month-old (bottom) WT and *Chd4*^{corin} mice.

(C) Chd4 immunohistochemistry (IHC) and picrosirius (picros.) staining in 8-week-old WT and *Chd4*^{corin} myocardium showing fibrosis of the interventricular septum (IVS) and left ventricle (LV) in mutant hearts. Arrowheads show nuclei of mutant cardiomyocytes free from Chd4 staining.

(D) Top: heart-weight-to-body-weight ratios (mg/g) in WT and *Chd4*^{corin} mice (n.s., not statistically significant; mean + SD). Bottom: histological staining with wheat germ agglutinin (WGA), showing no cardiomyocyte hypertrophy in mutant hearts.

(E) Cardiac ejection fraction measured in 8- to 12-week-old WT and *Chd4*^{corin} mice. ***$p \leq 0.001$ (mean + SD).

(F) Representative electrocardiography traces of representative (n = 7) 8- to 12-week-old WT and *Chd4*^{corin} mice.

were observed in *Chd4*-deficient E9.5 embryonic hearts (Figure S4E). To discard a differentiation of mutant cardiomyocytes along an inappropriate cell fate, we analyzed by IF the interstitial fibroblast marker Tcf4 in *Chd4*^{corin} mutant hearts. As expected in a diseased heart, *Chd4* mutant hearts present more fibrotic cells than WT, but these Tcf4-expressing cells do not express the cardiomyocyte marker α-actinin (Figure S5A). Moreover, we have analyzed the potential fibrogenic process of cultured isolated cardiomyocytes silenced for *Chd4* and found that these *Chd4*-silenced cardiomyocytes do not express fibrotic markers, further discarding a differentiation of *Chd4*-deficient cardiomyocytes along other cell fates (Figure S5B). These data demonstrate that *Chd4* inactivation in the heart derepresses the skeletal muscle terminal differentiation program and impairs the expression of genes required for ventricular chamber maturation.

expression of a randomly selected set of skeletal muscle genes upregulated in *Chd4* mutant hearts (Figure 3C), confirming that adult mutant cardiomyocytes expressed a larger number of skeletal muscle genes and to a larger extent than mutant embryonic cardiomyocytes. In situ hybridization (ISH) confirmed that *Gja5*, which encodes the gap junction channel connexin 40, was the most notably downregulated cardiovascular-related gene in *Chd4*^{Nkx} mutant hearts (Figure 3D). Similar to the results in adult mutant hearts, GSEA analysis showed that the skeletal muscle gene expression set was highly enriched in *Chd4*^{Nkx} hearts (Figure S4D). Immunohistochemical staining confirmed ectopic expression of Tnnt3 and Serca1 proteins in adult mutant hearts (Figures 3E and 3F). The transcriptional program during skeletal muscle differentiation is regulated by well-known myogenic factors such as *Myod1*, *Myog*, *Myf5*, and *Myf6* (Braun and Gautel, 2011), but no changes in gene expression of myogenic factors

Chd4 Represses the Cardiac Muscle Gene Program in Skeletal Muscle

We next tested the converse hypothesis that Chd4 might also regulate the maintenance of terminally differentiated skeletal muscle. We crossed *Chd4*^{floxed} mice with the Mck$^{cre/+}$ transgenic line to generate *Chd4*^{mck} mice, in which *Chd4* is ablated in mature skeletal muscle fibers (Brüning et al., 1998). Morphological comparison showed that the tibialis anterior (TA) muscle was significantly smaller and lighter in *Chd4*^{mck} mice than in WT littermates (Figure 4A). Histological analysis of *Chd4*^{mck} TA revealed fibers with central nuclei, expression of embryonic myosin heavy chain (eMHC or Myh3), and inflammatory infiltrate, features

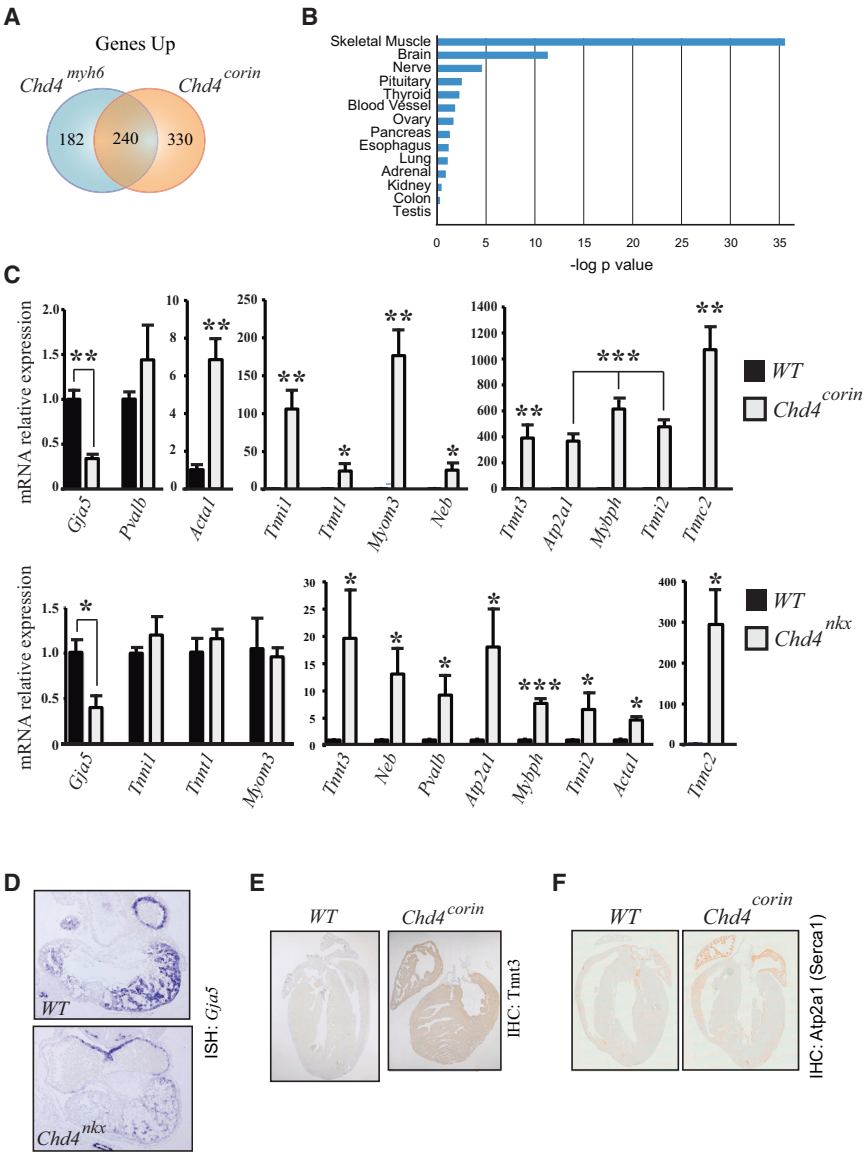

Figure 3. Chd4 Represses the Skeletal Muscle Terminal Differentiation Program in the Heart

(A) Venn diagram showing overlapping of genes identified in RNA-seq analysis as being significantly upregulated (fold change ≥ 2) in 2-week-old *Chd4*^{myh6} and 4-week-old *Chd4*^{corin} hearts versus WT.

(B) Tissue Specific Expression Analysis (TSEA) of the 240 common genes upregulated in both mutant hearts (*Chd4*^{myh6} and *Chd4*^{corin}), showing skeletal muscle and brain as the most represented tissues. Specificity index threshold (pSI) = 0.001.

(C) Quantitative PCR of a selection of deregulated genes in cardiac muscle of *Chd4*^{corin} 4-week-old mice (upper) and *Chd4*^{nkx} E10.5 hearts (lower), showing relative expression of mRNA with respect to WT (set at 1). *p ≤ 0.05, **p ≤ 0.005, and ***p ≤ 0.001 (mean + SD).

(D) ISH of connexin 40 (*Gja5*) in embryonic E10.5 WT and *Chd4*^{nkx} mutant hearts.

(E) IHC showing expression of skeletal muscle TnnT3 in WT and *Chd4*^{corin} hearts of 4-week-old mice. TnnT3 staining is an assembly of 7 pictures for WT and 8 pictures for *Chd4*^{corin}.

(F) IHC showing expression of skeletal muscle Serca1 (Atp2a1) in WT and *Chd4*^{corin} hearts.

indicative of altered muscle homeostasis and myopathy characterized by recurrent tissue degeneration and attempts at regeneration (Figure 4A). Additionally, *Chd4*^{mck} TA muscle showed aberrant staining for SDH and NADH, indicating disrupted mitochondrial activity and a further sign of muscle wasting (Figure 4B). Because the Mck$^{cre/+}$ transgene is expressed in terminally differentiated myofibers (and not in muscle stem cells or satellite cells), our results support a central role for Chd4 in maintaining homeostasis of mature skeletal muscle tissue.

To investigate how Chd4 exerts this skeletal muscle homeostatic function, we conducted RNA-seq analysis on TA muscles of 4-week-old WT and *Chd4*^{mck} mice. Global gene expression analysis identified 988 upregulated and 665 downregulated genes in *Chd4* mutant muscle (Table S2). Conversely to *Chd4*-deficient cardiac muscle, mutant skeletal muscle ectopically expressed transcripts of the cardiomyocyte lineage (Figures 4C and 4D). We corroborated the biological significance of this set of upregulated genes by GSEA and TSEA (Figures 4E and 4F and Table S3).

Chd4/NuRD Regulates Striated Muscle Genes by Direct Binding to Their Promoters and CpG Regions

We then checked by chromatin immunoprecipitation (ChIP) the binding of Chd4 to promoters of a selection of the most deregulated genes in both *Chd4* mutant hearts and *Chd4* mutant TA muscles. These experiments revealed binding of Chd4 to the selected promoters (Figure 5A). The Chd4/NuRD complex binds to a wide range of active and inactive promoters and to highly methylated loci (Menafra et al., 2014; Shimbo et al., 2013). We next examined potential differences in CpG methylation between cardiac and skeletal muscles by focusing on a group of genes regulated by Chd4 in each tissue. We first analyzed the CpG methylation status of these genes using cardiac and skeletal muscle genomic DNA and found significant differences in their DNA methylation status (Table S4). In general, we observed that cardiac genes display higher methylation levels in skeletal than in heart muscle and that skeletal muscle genes are more methylated in cardiac than in skeletal muscle (Table S4). We next conducted ChIP experiments to determine whether other NuRD complex subunits bind to the promoters and/or to the differentially methylated CpGs of the selected genes. These experiments revealed that Chd4, Mbd2, and/or Mbd3 and, to a lesser extent, Hdac1 occupy gene promoters and/or the CpG-containing regions of selected genes in cardiac tissue,

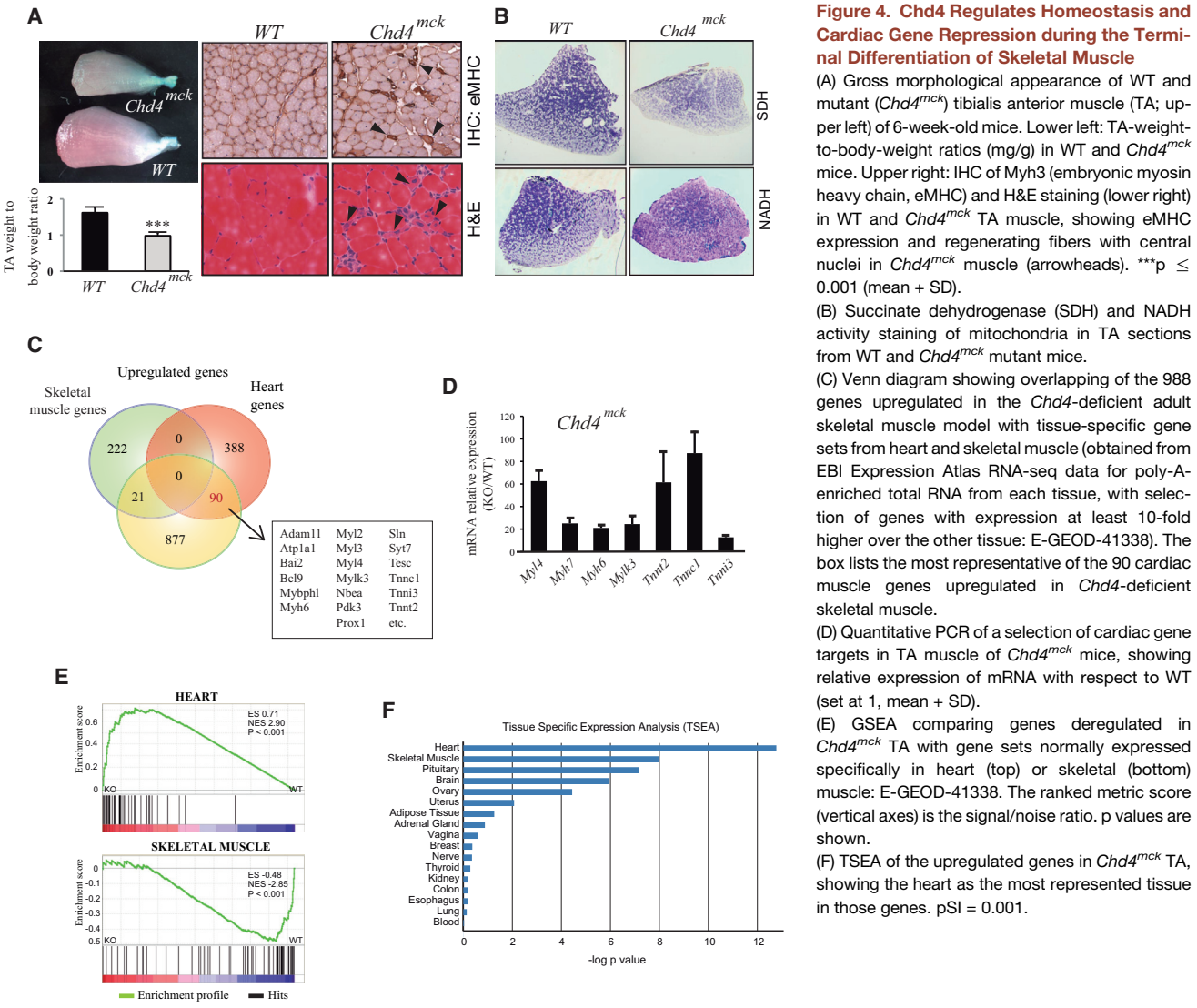

Figure 4. Chd4 Regulates Homeostasis and Cardiac Gene Repression during the Terminal Differentiation of Skeletal Muscle

(A) Gross morphological appearance of WT and mutant (*Chd4*^{mck}) tibialis anterior muscle (TA; upper left) of 6-week-old mice. Lower left: TA-weight-to-body-weight ratios (mg/g) in WT and *Chd4*^{mck} mice. Upper right: IHC of Myh3 (embryonic myosin heavy chain, eMHC) and H&E staining (lower right) in WT and *Chd4*^{mck} TA muscle, showing eMHC expression and regenerating fibers with central nuclei in *Chd4*^{mck} muscle (arrowheads). ***p $\leq$ 0.001 (mean + SD).

(B) Succinate dehydrogenase (SDH) and NADH activity staining of mitochondria in TA sections from WT and *Chd4*^{mck} mutant mice.

(C) Venn diagram showing overlapping of the 988 genes upregulated in the *Chd4*-deficient adult skeletal muscle model with tissue-specific gene sets from heart and skeletal muscle (obtained from EBI Expression Atlas RNA-seq data for poly-A-enriched total RNA from each tissue, with selection of genes with expression at least 10-fold higher over the other tissue: E-GEOD-41338). The box lists the most representative of the 90 cardiac muscle genes upregulated in *Chd4*-deficient skeletal muscle.

(D) Quantitative PCR of a selection of cardiac gene targets in TA muscle of *Chd4*^{mck} mice, showing relative expression of mRNA with respect to WT (set at 1, mean + SD).

(E) GSEA comparing genes deregulated in *Chd4*^{mck} TA with gene sets normally expressed specifically in heart (top) or skeletal (bottom) muscle: E-GEOD-41338. The ranked metric score (vertical axes) is the signal/noise ratio. p values are shown.

(F) TSEA of the upregulated genes in *Chd4*^{mck} TA, showing the heart as the most represented tissue in those genes. pSI = 0.001.

confirming direct interaction of the Chd4/NuRD complex (Figures 5B and S5C). This interaction was not detected in *Chd4*^{corin} hearts and was greatly reduced in regions other than promoters or CpGs-containing regions of the tested genes (Figure 5B). In agreement with this, Chd4 and the other components of the NuRD complex were found to bind to promoters and CpGs-containing sequences of cardiac genes in terminally differentiated skeletal myofibers (Figures 5C and S5D). Together, these data indicate that Chd4/NuRD controls mature striated muscle identity by directly repressing the terminal differentiation program of the skeletal muscle lineage in differentiated cardiomyocytes and, reciprocally, repressing the terminal differentiation program of the cardiac muscle lineage in skeletal muscle. Notably, individual silencing of components of the NuRD complex in cardiomyocytes revealed that derepression of skeletal muscle genes in adult cardiomyocytes was achieved only when *Chd4* was silenced (Figure S6), suggesting that the helicase Chd4 is the main component of the NuRD complex needed to maintain skeletal muscle genes repressed in the heart.

The Chd4/NuRD Complex Regulates Mitochondrial Homeostasis in Striated Muscle

In *Chd4*-deficient skeletal muscle, most of the downregulated genes are linked to mitochondrial processes. In particular, most of the mtDNA-encoded genes, all devoted to the biogenesis of the oxidative phosphorylation (OXPHOS) system, are strongly downregulated, indicating an alteration in energy homeostasis (Figure 6A and Table S2). Consistent with this, the master regulator of mitochondrial biogenesis *Pgc1*α is strongly downregulated. In mutant hearts, however, the number of downregulated mitochondrial transcripts was significantly lower, and neither *Pgc1a* nor any of the OXPHOS structural genes, whether mtDNA- or nDNA-encoded, are significantly affected (Figure S3F and Table S1). We confirmed these data by quantitative PCR in mutant striated muscles (Figures 6B and S7A). Important proteins downregulated in both tissues include the mitochondrial protein deacetylase Sirt5, required for posttranslational modification of mitochondrial proteins, and the mitochondrial intermediate peptidase Mipep, a

fundamental component of the mitochondrial protein import machinery.

We next analyzed the methylation status of the promoters of a selected set of common deregulated mitochondrial genes in both striated muscles and found slight, but significant, differences in the same direction as above (Table S4). ChIP experiments revealed that Chd4/NuRD binds to the respective promoter regions of *Mipep*, *Pgc1a*, *Sirt5*, and *Ucp2* genes in both striated muscles (Figures 6C and 6D), confirming that the Chd4/NuRD complex controls the expression of mitochondria-related genes by directly binding to their promoters.

We then investigated the consequences of the mitochondrial transcriptional deregulation in *Chd4* mutant striated muscles. We first inquired if mitochondrial mass per cell was affected in *Chd4*-deficient muscle. Indeed, citrate synthase (CS) and cytochrome oxidase (COX) enzymatic activities, and therefore mitochondrial mass, were reduced in *Chd4*-deficient skeletal muscle but not in heart (Figure 7A). In addition, ATP production in isolated mitochondria was decreased in *Chd4*-deficient hearts but remained unchanged in mutant skeletal muscle (Figure 7B). The functional observations were in agreement with the decrease in *Pgc1a* and mitochondrial transcripts in the skeletal muscle but not in the heart (Arany et al., 2005). Thus, either by reducing mitochondrial mass (skeletal muscle) or by reducing the efficacy of ATP synthesis by mitochondria (heart), the mitochondrial ATP synthesis capacity in *Chd4*-deficient striated muscle is reduced. Ultrastructurally, mitochondria were more elongated in both tissues as revealed by higher abundance of the long isoforms of OPA1 (Figure 7C), possibly providing a compensatory mechanism to prevent excessive mitophagy (Gomes et al., 2011; Patten et al., 2014). The decrease in mitochondrial ATP synthesis potential can be consequence of the reduction of the mitochondrial electron transport chain or of the ATP synthase capacity. We did not observe changes in mitochondrial respiratory complex amount or distribution between complexes and supercomplexes in the mutant tissues (Figure S7B). In contrast, the bioenergetic index of the cell (or BEC index), defined as the ATP5b/GAPDH ratio (Cuezva et al., 2002), was decreased, indicating an overall reduction in oxidative potential in favor of glycolysis for the ATP production by the cell (Figures 7D and S7C).

DISCUSSION

Here we demonstrate an essential function of the chromatin remodeling Chd4/NuRD complex in the control of striated muscle tissue identity and metabolic homeostasis. Chd4/NuRD controls heart muscle identity by silencing the skeletal muscle lineage gene program. Inactivation of *Chd4* in cardiomyocytes causes inappropriate expression of skeletal muscle genes accompanied by prominent fibrosis, as well as a severe cardiomyopathy, with reduction in the cardiac ejection fraction, arrhythmia, and sudden death. Conversely, deletion of *Chd4* in skeletal muscle leads to derepression of cardiac muscle genes and concomitant myopathy. These findings identify Chd4/NuRD as a reciprocal regulator of heart and skeletal muscle identities. Furthermore, Chd4/NuRD is also required for metabolic homeostasis in both tissues by direct epigenetic regulation of mitochondrial genes.

The NuRD complex components Hdac1 and 2 were previously found to repress the expression of some skeletal muscle genes in the heart (Montgomery et al., 2007), with no reciprocal effect in skeletal muscle (Moresi et al., 2012). No other component of the NuRD complex has been conditionally deleted in cardiac or skeletal muscles. Our findings thus reveal the functional specificity of the NuRD complex element Chd4 for the alternate fates of striated muscle. Despite the presence of the NuRD complex subunits Mbd2, Mbd3, and Hdac1 in the regulatory regions of the derepressed genes, Chd4 appears to be the main contributor to the repression exerted by the complex, as shown by functional silencing of individual subunits. Chd4/NuRD also binds to differentially methylated CpG-containing regions, supporting the implication of the additional NuRD components in the initial recruitment of Chd4, rather than the active repression at the differentiated state.

Chd4/NuRD is a well-known transcriptional repressor in stem cell biology and differentiation. Although NuRD has been shown to be required to maintain lineage fidelity throughout megakaryocyte-erythroid ontogeny, virtually nothing is known about its role in tissue homeostasis (Gregory et al., 2010). Our results show that cardiac and skeletal muscles, despite their different ontogeny, maintain an exquisite transcriptional control of their respective myofibrilar sarcomeric components in a NuRD-dependent manner. Perturbation of this control has dramatic functional consequences, leading to "hybrid" striated muscle tissues that resemble human heart and skeletal muscle disease states and are incompatible with life. These findings challenge the prevailing idea that the NuRD complex exclusively regulates embryonic stem cell biology and cell differentiation (Signolet and Hendrich, 2015).

Our results also show that Chd4/NuRD, by positively regulating the expression of mitochondrial genes, is an essential regulator of mitochondrial homeostasis whose loss leads to insufficient mitochondrial ATP synthesis in both heart and skeletal muscle, contributing to the disease phenotype. These results are in line with the recently described binding of Chd4 and other helicases to active promoters in association with the general transcription machinery (de Dieuleveult et al., 2016). Interestingly, the origin of the bioenergetic deficiency in each tissue is slightly different. In skeletal muscle we observed an overall decrease in mitochondrial mass per cell, but ATP synthesis capacity per mitochondria was maintained. In contrast, in heart mitochondrial mass per cell was maintained and mitochondrial ATP synthesis capacity reduced. This difference might be due to the distinct number and nature of Chd4/NuRD-dependent genes in each tissue. Thus, the Chd4/NuRD complex plays a critical role in maintaining lineage identity and metabolic homeostasis of striated muscles by both repressing and inducing epigenetic activities.

EXPERIMENTAL PROCEDURES

Mice, Embryos, and Genotyping

The *Chd4* ^{floxed} mouse strain has been previously described (Williams et al., 2004). The transgenic Cre mouse strains used were *Nkx2.5* $^{cre/+}$, *cTnT* $^{cre/+}$, *α-MHC* $^{cre/+}$, *Corin* $^{cre/cre}$, and *Mck* $^{cre/+}$, all of them previously described (Agah et al., 1997; Brüning et al., 1998; Enshell-Seijffers et al., 2010; Jiao et al., 2003; Stanley et al., 2002). Welfare of animals used for experimental and other scientific purposes conformed to EU Directive 2010/63EU and

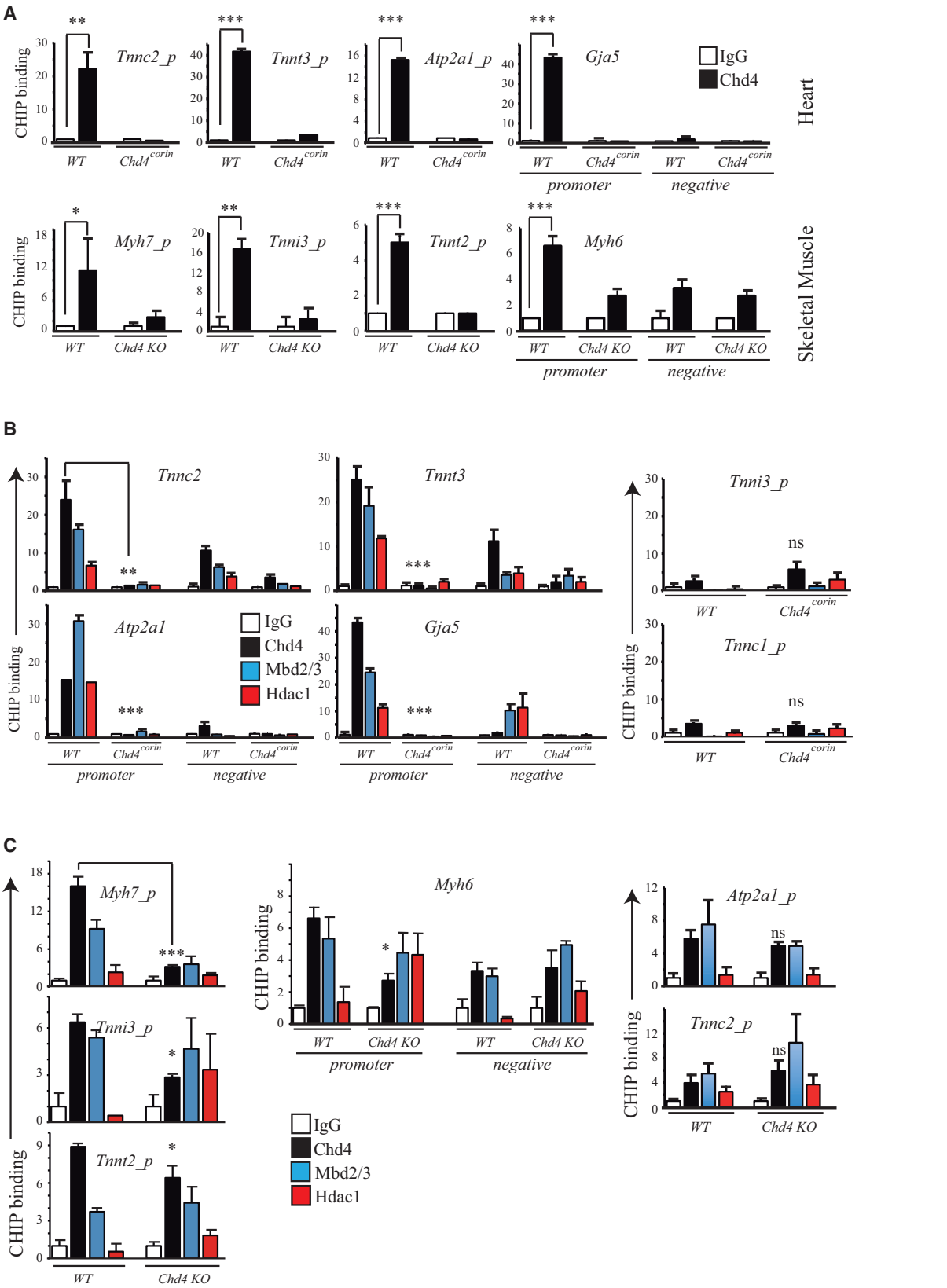

(legend on next page)

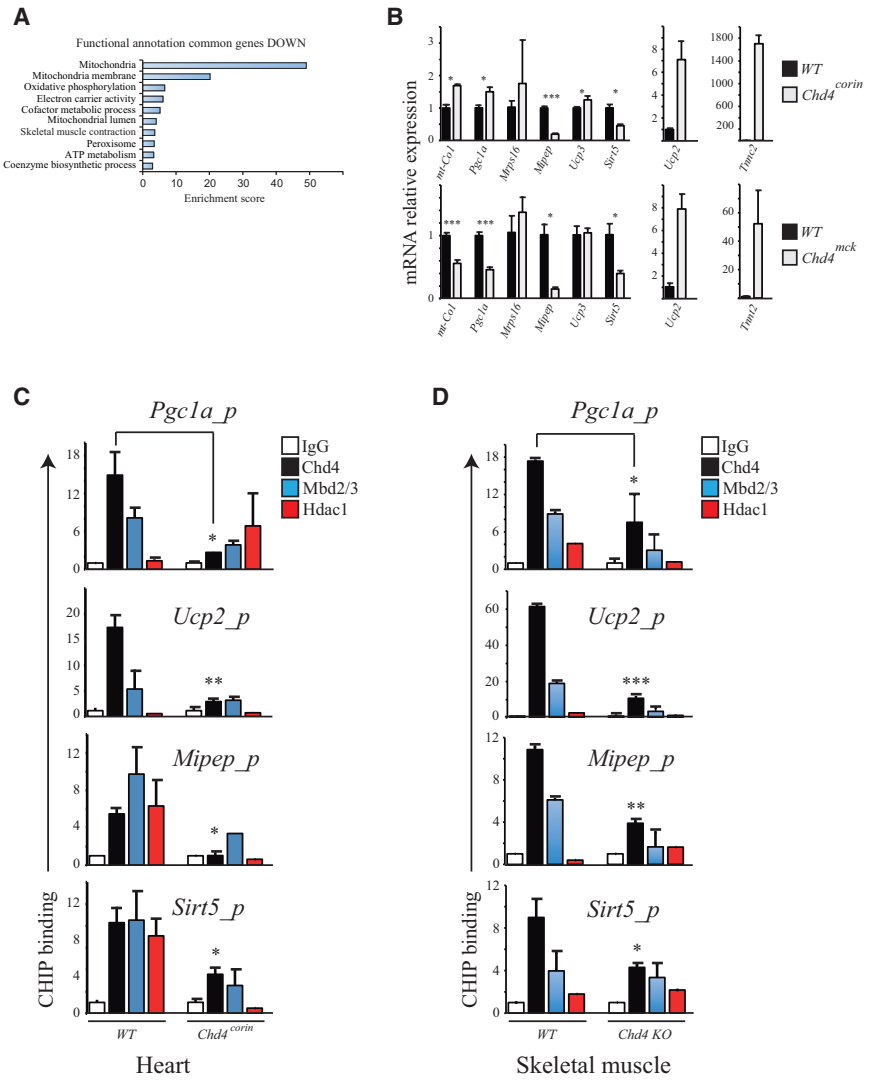

Figure 6. Chd4/NuRD Regulates the Mitochondrial Gene Program in Striated Muscle

(A) Functional annotation analysis of GO performed in DAVID to identify biological processes enriched in the downregulated gene set in *Chd4*^{mck} skeletal muscle. The top annotation clusters are shown according to their enrichment score; names are based on enriched GO annotations.

(B) Quantitative PCR of a selection of mitochondrial gene targets in hearts of 4-week-old WT and *Chd4*^{corin} mice (top) and in TA muscles of 4-week-old *WT* and *Chd4*^{mck} mice (bottom). *Tnnc2* (top) and *Tnnt2* (bottom) are shown as upregulated gene controls in mutant cardiac and skeletal muscle, respectively. *p $\leq$ 0.05 and ***p $\leq$ 0.001 (bars show mean + SD).

(C and D) ChIP experiments in WT and *Chd4*^{corin} hearts (C) and WT and *Chd4 KO*-derived myofibers (D) for IgG (control), Chd4, Mbd2/3, and Hdac1, with qPCR for proximal promoters of mitochondrial genes *Pgc1a* (*Pgc1a_p*), *Ucp2* (*Ucp2_p*), *Mipep* (*Mipep_p*), and *Sirt5* (*Sirt5_p*). Results are plotted relative to IgG (set at 1). *p $\leq$ 0.05, **p $\leq$ 0.005, and ***p $\leq$ 0.001 (mean + SD).

Recommendation 2007/526/EC, enforced in Spanish law under Real Decreto 53/2013. Experiments with mice and embryos were approved by the CNIC Animal Experimentation Ethics Committee.

Histological Analysis

Embryo and adult hearts were fixed overnight in 4% paraformaldehyde in PBS, embedded in paraffin, and cut with a microtome. Sections were stained with hematoxylin and eosin (H&E) using standard procedures. Muscles were frozen in liquid nitrogen, embedded in OCT, and then cut on a cryotome. Immunohistochemistry (IHC), immunofluorescence (IF), and mitochondrial activity (SDH and NADH) were performed using standard procedures. RNA in situ hybridization (ISH) was performed with digoxigenin RNA probes using standard procedures. The histological images were acquired as described in the Supplemental Experimental Procedures.

Cell Culture and Adenoviral Transduction

Satellite cells from *Chd4*^{floxed} mice were isolated by FACS as previously described (Sousa-Victor et al., 2014) and maintained in Ham's F10 supplemented with 20% FBS and bFGF (0.025 μg/ml) (growth medium, GM). To induce differentiation, GM was replaced with differentiation medium (DM; DMEM supplemented with 2% horse serum) at myoblast subconfluence. At 24 hr of differentiation, myotubes were transduced with Ad-GFP or Ad-CRE, and cells were incubated in DM for an additional 48 hr.

Cardiomyocyte Proliferation

Cardiomyocyte proliferation was analyzed by IHC staining of Ki67 on E11.5 embryonic sections. Total ventricular compact wall cardiomyocytes and Ki67-positive cardiomyocytic nuclei were counted in at least five sections from 4–5 embryos of each genotype, obtained from at least two mothers (p $\leq$ 0.01, mean + SD).

Figure 5. Chd4/NuRD Regulates Skeletal Muscle Genes in Cardiomyocytes and Cardiac Genes in Skeletal Muscle by Direct Binding to Their Gene Regulatory Regions

(A) Upper graphs: ChIP experiments in WT and *Chd4*^{corin} hearts for IgG (control) and Chd4, with qPCR for proximal promoters of *Tnnc2* (*Tnnc2_p*), *Tnnt3* (*Tnnt3_p*), *Atp2a1* (*Atp2a1_p*), and *Gja5* (promoter), and a *Gja5* genic negative control. Lower graphs: ChIP experiments in WT and *Chd4 KO*-derived myotubes with qPCR for proximal promoters of *Myh7* (*Myh7_p*), *Tnni3* (*Tnni3_p*), *Tnnt2* (*Tnnt2_p*), and *Myh6* (promoter), and an additional *Myh6* sequence, as a negative control.

(B) ChIP experiments in WT and *Chd4*^{corin} hearts for IgG (control), Chd4, Mbd2/3, and Hdac1, with qPCR for proximal promoters of *Tnnc2*, *Tnnt3*, *Atp2a1*, and *Gja5*. Binding to regions near the gene bodies are shown as negative controls (Table S4). The cardiac genes *Tnni3* and *Tnnc1* are shown as controls (right).

(C) ChIP experiments in WT and *Chd4 KO*-derived myotubes for IgG (control), Chd4, Mbd2/3, and Hdac1, with qPCR for the indicated proximal promoters, with a negative region near the promoter of *Myh6* (Table S4). The skeletal muscle genes *Atp2a1* and *Tnnc2* are shown as controls.

Representative experiments are shown out of 5 (A), 3 (B), and 3 (C) with similar results. ns, not statistically significant, *p $\leq$ 0.05, **p $\leq$ 0.005 and ***p $\leq$ 0.001, bars show mean + SD. All results are plotted relative to IgG (set at 1).

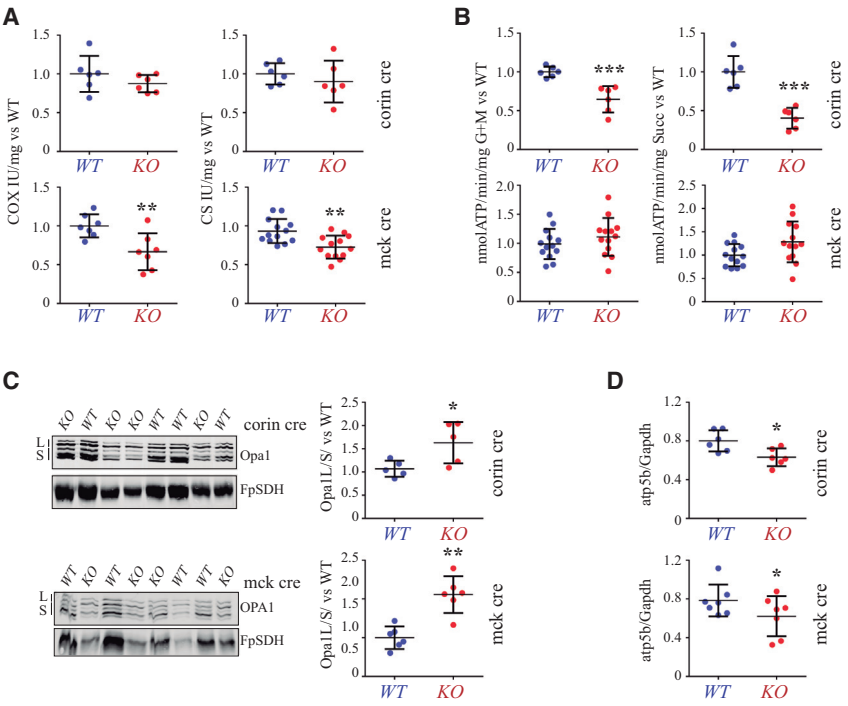

Figure 7. Chd4/NuRD Controls Mitochondrial Function in Striated Muscle

(A) Cytochrome *c* oxidase (COX, left panels) and citrate synthase (CS, right panels) activities in cell homogenates from WT and *Chd4*^{corin} (KO) hearts (upper panels, corin cre) and of WT and *Chd4*^{mck} (KO) TA (lower panels, mck cre) of 4-week-old mice.

(B) ATP synthesis in mitochondria isolated from WT and *Chd4*^{corin} (KO) hearts (upper panels, corin cre) and of WT and *Chd4*^{mck} TA (lower panels, mck cre).

(C) Western blot of OPA1 expression in isolated mitochondria of WT and *Chd4*^{corin} (KO) hearts (upper left panel, corin cre) and of WT and *Chd4*^{mck} TA (lower left panel, mck cre), with corresponding measurements of the large (L) OPA1 to short (S) OPA1 isoform ratio (right panels).

(D) Atp5b:Gapdh expression ratio in WT and *Chd4*^{corin} (KO) hearts (upper panel, corin cre) and in WT and *Chd4*^{mck} (KO) TA (lower panel, mck cre). Data correspond to the blots of Figure S7C. *p $\leq$ 0.05, **p $\leq$ 0.005, and ***p $\leq$ 0.001 (mean ± SD).

Adult Cardiomyocyte RNA Silencing

For adult cardiomyocyte isolation, aorta from surgically excised heart was cannulated onto a perfusion system with calcium-free perfusion buffer, and the cardiomyocytes were enzymatically disassociated using Liberase DH (Roche). Digestion was terminated with 10% FCS and 12.5 μM $CaCl_2$. Isolated cardiomyocytes were cultured in laminin-coated dishes in growth media (GM; Medium 199 with Earle's salt supplemented with Creatinine [5 mM], L-Carnitine [2 mM], Taurin [5 mM], Insulin Transferrin Selenium [1X ITS-G], 2% fetal bovine serum, 1% penicillin/streptomycin, and 25 mM HEPES [pH7.3]). Media was exchanged 2 hr post seeding to remove dead cells and erythrocytes. RNAi silencing against the NuRD components was performed using smart pool siRNAs from Dharmacon as described by the manufacturer's protocol in GM without serum and penicillin/streptomycin. The cardiomyocytes were harvested 72 hr post transfection for RNA extraction using Trizol reagent (Thermo Fisher Scientific) according to the manufacturer's protocol.

Chromatin Immunoprecipitation

Chromatin immunoprecipitation (ChIP) was performed as previously described (Shen et al., 2012). Briefly, hearts from 4-week-old WT or *Chd4*^{corin} mice were dissected and minced with a sterile blade, and the tissue was disrupted in a Dounce homogenizer. Cells were filtered through a 100 μM strainer and formaldehyde cross-linked. The cross-linked cardiomyocytes were then lysed, and chromatin was sheared by sonication using a Bioruptor ultrasonicator (Diagenode). Sheared chromatin was immunoprecipitated with a 1:1 equimolar mix of antibodies to Chd4 (ab70469 and ab72418, Abcam), a 1:1:1 mix of antibodies to Mbd2/3 (ab45027, Abcam; A301-632A, Bethyl; M7318, Sigma), a 1:1 mix of antibodies to Hdac1 (ab46985, Abcam; sc-6298X, Santa Cruz), or control IgG (Cell Signaling 2729). DNA was isolated and analyzed by qPCR. Primer sequences and genomic locations are provided in Table S4.

For myofiber ChIP, differentiated myotubes were formaldehyde cross-linked and lysed, and chromatin was sheared by sonication. Sonicated chromatin was then subjected to immunoprecipitation as above. DNA was isolated and analyzed by qPCR using specific primer sets (Table S4).

Bisulfite Modification and Pyrosequencing

Genomic DNA isolated from mouse cardiac and skeletal muscle tissue was bisulfite converted using the EZ DNA Methylation Kit (Zymo Research). 20–30 ng of modified DNA was used as a template in each subsequent PCR. Primers for PCR amplification (Table S4) and pyrosequencing were designed with PyroMark Assay Design 2.0 (QIAGEN). PCR was performed with the HotStart Taq DNA polymerase PCR Kit (QIAGEN), and the amplification was confirmed by agarose gel electrophoresis. PCR products were pyrosequenced with the Pyromark Q24 system (QIAGEN). Results from bisulfite pyrosequencing are presented as a percentage of methylation.

Echocardiography and Electrocardiography

Echocardiography and ECG recordings were obtained as previously described (Luxán et al., 2013).

RNA Sequencing and Statistical Analysis

For transcription profiling of adult organs, hearts were surgically isolated from 3-week-old WT and *Chd4*^{corin} mice and TA muscles from 4-week-old WT and *Chd4*^{mck} mice. Organs were individually introduced into 1 ml TRIsure buffer (Bioline), immediately snap-frozen in liquid N_2, and stored at −80°C. Tissue was homogenized with the MagNA lyser system (Roche) and total RNA isolated. RNA was pooled from 3–4 hearts per genotype and purified on QIAGEN-RNA-clean columns (QIAGEN). Experiments were performed in triplicate (3 WT and 3 mutant pools). For profiling of embryonic hearts, individual E10.5 hearts were suspended in 100 μl TRIsure buffer (Bioline). Ten WT or *Chd4*^{nkx} hearts from 3–5 different mothers were then pooled, and total RNA was extracted and cleaned. The experiment was performed in triplicate. The samples were treated in the same way as the adult hearts. RNA sequencing is described in the Supplemental Experimental Procedures.

Statistical analyses results are expressed as mean + SD. The significance of differences between WT and corresponding mutant groups was assessed by two-tail Student's t test or χ^2 as noted. Statistical significance was set at a p value < 0.05.

Isolation of Mitochondria, OXPHOS Function, Enzyme Activities, SDS, and Blue Native Electrophoresis Analysis

Mitochondria were isolated from cell lines or mouse hearts as described (Fernández-Vizarra et al., 2002).

ATP synthesis in isolated mitochondria (15–25 μg mitochondrial protein) was measured using a kinetic luminescence assay (Vives-Bauza et al., 2007). Mitochondrial fractions were prepared and the activities of individual complexes measured spectrophotometrically (Birch-Machin and Turnbull, 2001).

Bioenergetic index in cell homogenates and mitochondrial dynamics in isolated mitochondria were analyzed by Western blot after SDS-PAGE (Cuezva et al., 2002). Supercomplex levels and composition were analyzed

in isolated heart mitochondria by blue native electrophoresis (Acín-Pérez et al., 2008). Protein levels were assessed using antibodies to the following proteins: FpSDH (Novex); OPA1, GAPDH, and core1 (Abcam); and ATP5B (MitoSciences).

SUPPLEMENTAL INFORMATION

Supplemental Information includes Supplemental Experimental Procedures, seven figures, and four tables and can be found with this article online at http://dx.doi.org/10.1016/j.cmet.2016.04.008.

AUTHOR CONTRIBUTIONS

P.G.A. and J.M.R. conceived the project. P.G.A. designed and performed most of the experiments. E.P., P.S.Y.-L., R.A.-P., M.Z., A.G.-G., K.S., M.J.-A., J.S., D.L.-M., B.O., G.D., and J.K. also performed experiments. E.P. and A.B.M.M.K.I. performed gene ontology and in silico transcription factor binding analysis. E.P. performed GSEA and TSEA. Results were analyzed by P.G.A. and J.M.R., with help from E.P., P.S.Y.-L., R.A.-P., M.Z., A.G.-G., J.S., L.J.J.-B., J.L.P., J.A.E., E.B., and P.M.-C. D.E.-S., B.M., and K.G. generated the corin Cre line and helped in its initial phenotypic characterization. P.G.A. and J.M.R. wrote the paper, with significant contributions from E.P., R.A.-P., A.G.-G., J.L.P., J.A.E., E.B., and P.M.-C. Specific sections were written with help from L.J.J.-B., A.B.M.M.K.I., K.G., J.K., and T.B.

ACKNOWLEDGMENTS

We thank Drs. Richard Harvey (University of Sydney, Australia) and Michael Schneider (Imperial College, London, UK) for providing *Nkx2.5*$^{cre/+}$ and α-*MHC* $^{cre/+}$ transgenic lines, respectively, Dr. S. Bartlett for English editing, and Gemma Benito and Ana Guío for technical assistance. J.M.R. is supported by the Spanish Ministry of Economy and Competitiveness (Ministerio de Economía y Competitividad; SAF 2012 34296 and SAF 2015 63633-R), the Spanish Ministry of Health (Ministerio de Sanidad y Consumo) Red de Investigación Cardiovascular (RIC; grant RD06/0042/0022), and the Fundación La Marató TV3 (264/C/2012). The RIC also supports J.L.P. (RD12/0042/0005) and L.J.J.-B. (RD12/0042/0056). RIC grants are partially funded by FEDER funds. P.M.-C., J.A.E., and J.L.P. are supported by SAF2012-38547, SAF2015-67369-R, SAF2012-1207, and SAF2013-45543-R, respectively. E.P. and P.M.-C. were also supported by SAF2015-67369-R. NGS experiments were performed at the CNIC Genomics Unit. IF of adult hearts was performed at the Advanced Fluorescence Microscopy Unit of (IBMB-CSIC) Barcelona. The CNIC is supported by the Spanish Ministry of Economy and Competitiveness and the Pro-CNIC Foundation and is a Severo Ochoa Center of Excellence (MINECO award SEV-2015-0505). R.A.-P. was supported by a Ramón y Cajal grant and is a holder of a Marie Curie grant (RA-P: UEO/MCA1108). M.Z. was a holder of a Marie Curie Outgoing International Fellowship (MOIF-CT-2006-039327), and P.G.A. was supported by a Ramón y Cajal grant from the Spanish Ministry of Education, Science and Sport.

Received: June 26, 2015
Revised: February 19, 2016
Accepted: April 13, 2016
Published: May 10, 2016

REFERENCES

Acín-Pérez, R., Fernández-Silva, P., Peleato, M.L., Pérez-Martos, A., and Enriquez, J.A. (2008). Respiratory active mitochondrial supercomplexes. Mol. Cell *32*, 529–539.

Agah, R., Frenkel, P.A., French, B.A., Michael, L.H., Overbeek, P.A., and Schneider, M.D. (1997). Gene recombination in postmitotic cells. Targeted expression of Cre recombinase provokes cardiac-restricted, site-specific rearrangement in adult ventricular muscle in vivo. J. Clin. Invest. *100*, 169–179.

Arany, Z., He, H., Lin, J., Hoyer, K., Handschin, C., Toka, O., Ahmad, F., Matsui, T., Chin, S., Wu, P.H., et al. (2005). Transcriptional coactivator PGC-1 alpha controls the energy state and contractile function of cardiac muscle. Cell Metab. *1*, 259–271.

Asp, P., Blum, R., Vethantham, V., Parisi, F., Micsinai, M., Cheng, J., Bowman, C., Kluger, Y., and Dynlacht, B.D. (2011). Genome-wide remodeling of the epigenetic landscape during myogenic differentiation. Proc. Natl. Acad. Sci. USA *108*, E149–E158.

Birch-Machin, M.A., and Turnbull, D.M. (2001). Assaying mitochondrial respiratory complex activity in mitochondria isolated from human cells and tissues. Methods Cell Biol. *65*, 97–117.

Braun, T., and Gautel, M. (2011). Transcriptional mechanisms regulating skeletal muscle differentiation, growth and homeostasis. Nat. Rev. Mol. Cell Biol. *12*, 349–361.

Bruneau, B.G. (2010). Chromatin remodeling in heart development. Curr. Opin. Genet. Dev. *20*, 505–511.

Brüning, J.C., Michael, M.D., Winnay, J.N., Hayashi, T., Hörsch, D., Accili, D., Goodyear, L.J., and Kahn, C.R. (1998). A muscle-specific insulin receptor knockout exhibits features of the metabolic syndrome of NIDDM without altering glucose tolerance. Mol. Cell *2*, 559–569.

Buckingham, M., and Rigby, P.W. (2014). Gene regulatory networks and transcriptional mechanisms that control myogenesis. Dev. Cell *28*, 225–238.

Chang, C.P., and Bruneau, B.G. (2012). Epigenetics and cardiovascular development. Annu. Rev. Physiol. *74*, 41–68.

Cuezva, J.M., Krajewska, M., de Heredia, M.L., Krajewski, S., Santamaria, G., Kim, H., Zapata, J.M., Marusawa, H., Chamorro, M., and Reed, J.C. (2002). The bioenergetic signature of cancer: a marker of tumor progression. Cancer Res *62*, 6674–6681.

de Dieuleveult, M., Yen, K., Hmitou, I., Depaux, A., Boussouar, F., Bou Dargham, D., Jounier, S., Humbertclaude, H., Ribierre, F., Baulard, C., et al. (2016). Genome-wide nucleosome specificity and function of chromatin remodellers in ES cells. Nature *530*, 113–116.

Dennis, G., Jr., Sherman, B.T., Hosack, D.A., Yang, J., Gao, W., Lane, H.C., and Lempicki, R.A. (2003). DAVID: Database for Annotation, Visualization, and Integrated Discovery. Genome Biol. *4*, 3.

Enshell-Seijffers, D., Lindon, C., Kashiwagi, M., and Morgan, B.A. (2010). beta-catenin activity in the dermal papilla regulates morphogenesis and regeneration of hair. Dev. Cell *18*, 633–642.

Estrella, N.L., and Naya, F.J. (2014). Transcriptional networks regulating the costamere, sarcomere, and other cytoskeletal structures in striated muscle. Cell. Mol. Life Sci. *71*, 1641–1656.

Fan, W., and Evans, R. (2015). PPARs and ERRs: molecular mediators of mitochondrial metabolism. Curr. Opin. Cell Biol. *33*, 49–54.

Fernández-Vizarra, E., López-Pérez, M.J., and Enriquez, J.A. (2002). Isolation of biogenetically competent mitochondria from mammalian tissues and cultured cells. Methods *26*, 292–297.

Gomes, L.C., Di Benedetto, G., and Scorrano, L. (2011). During autophagy mitochondria elongate, are spared from degradation and sustain cell viability. Nat. Cell Biol. *13*, 589–598.

Gregory, G.D., Miccio, A., Bersenev, A., Wang, Y., Hong, W., Zhang, Z., Poncz, M., Tong, W., and Blobel, G.A. (2010). FOG1 requires NuRD to promote hematopoiesis and maintain lineage fidelity within the megakaryocytic-erythroid compartment. Blood *115*, 2156–2166.

Hu, G., and Wade, P.A. (2012). NuRD and pluripotency: a complex balancing act. Cell Stem Cell *10*, 497–503.

Jiao, K., Kulessa, H., Tompkins, K., Zhou, Y., Batts, L., Baldwin, H.S., and Hogan, B.L. (2003). An essential role of Bmp4 in the atrioventricular septation of the mouse heart. Genes Dev. *17*, 2362–2367.

Kashiwagi, M., Morgan, B.A., and Georgopoulos, K. (2007). The chromatin remodeler Mi-2beta is required for establishment of the basal epidermis and normal differentiation of its progeny. Development *134*, 1571–1582.

Lai, A.Y., and Wade, P.A. (2011). Cancer biology and NuRD: a multifaceted chromatin remodelling complex. Nat. Rev. Cancer *11*, 588–596.

Laugesen, A., and Helin, K. (2014). Chromatin repressive complexes in stem cells, development, and cancer. Cell Stem Cell *14*, 735–751.

Le Guezennec, X., Vermeulen, M., Brinkman, A.B., Hoeijmakers, W.A., Cohen, A., Lasonder, E., and Stunnenberg, H.G. (2006). MBD2/NuRD and MBD3/NuRD, two distinct complexes with different biochemical and functional properties. Mol. Cell. Biol. *26*, 843–851.

Luxán, G., Casanova, J.C., Martínez-Poveda, B., Prados, B., D'Amato, G., MacGrogan, D., Gonzalez-Rajal, A., Dobarro, D., Torroja, C., Martinez, F., et al. (2013). Mutations in the NOTCH pathway regulator MIB1 cause left ventricular noncompaction cardiomyopathy. Nat. Med. *19*, 193–201.

Mathiyalagan, P., Keating, S.T., Du, X.J., and El-Osta, A. (2014). Chromatin modifications remodel cardiac gene expression. Cardiovasc. Res. *103*, 7–16.

Menafra, R., Brinkman, A.B., Matarese, F., Franci, G., Bartels, S.J., Nguyen, L., Shimbo, T., Wade, P.A., Hubner, N.C., and Stunnenberg, H.G. (2014). Genome-wide binding of MBD2 reveals strong preference for highly methylated loci. PLoS ONE *9*, e99603.

Montgomery, R.L., Davis, C.A., Potthoff, M.J., Haberland, M., Fielitz, J., Qi, X., Hill, J.A., Richardson, J.A., and Olson, E.N. (2007). Histone deacetylases 1 and 2 redundantly regulate cardiac morphogenesis, growth, and contractility. Genes Dev. *21*, 1790–1802.

Moresi, V., Carrer, M., Grueter, C.E., Rifki, O.F., Shelton, J.M., Richardson, J.A., Bassel-Duby, R., and Olson, E.N. (2012). Histone deacetylases 1 and 2 regulate autophagy flux and skeletal muscle homeostasis in mice. Proc. Natl. Acad. Sci. USA *109*, 1649–1654.

Naito, T., Gómez-Del Arco, P., Williams, C.J., and Georgopoulos, K. (2007). Antagonistic interactions between Ikaros and the chromatin remodeler Mi-2beta determine silencer activity and Cd4 gene expression. Immunity *27*, 723–734.

O'Shaughnessy, A., and Hendrich, B. (2013). CHD4 in the DNA-damage response and cell cycle progression: not so NuRDy now. Biochem. Soc. Trans. *41*, 777–782.

O'Shaughnessy-Kirwan, A., Signolet, J., Costello, I., Gharbi, S., and Hendrich, B. (2015). Constraint of gene expression by the chromatin remodelling protein CHD4 facilitates lineage specification. Development *142*, 2586–2597.

Patten, D.A., Wong, J., Khacho, M., Soubannier, V., Mailloux, R.J., Pilon-Larose, K., MacLaurin, J.G., Park, D.S., McBride, H.M., Trinkle-Mulcahy, L., et al. (2014). OPA1-dependent cristae modulation is essential for cellular adaptation to metabolic demand. EMBO J. *33*, 2676–2691.

Reynolds, N., Latos, P., Hynes-Allen, A., Loos, R., Leaford, D., O'Shaughnessy, A., Mosaku, O., Signolet, J., Brennecke, P., Kalkan, T., et al. (2012). NuRD suppresses pluripotency gene expression to promote transcriptional heterogeneity and lineage commitment. Cell Stem Cell *10*, 583–594.

Segalés, J., Perdiguero, E., and Muñoz-Cánoves, P. (2015). Epigenetic control of adult skeletal muscle stem cell functions. FEBS J. *282*, 1571–1588.

Shen, Y., Yue, F., McCleary, D.F., Ye, Z., Edsall, L., Kuan, S., Wagner, U., Dixon, J., Lee, L., Lobanenkov, V.V., and Ren, B. (2012). A map of the cis-regulatory sequences in the mouse genome. Nature *488*, 116–120.

Shimbo, T., Du, Y., Grimm, S.A., Dhasarathy, A., Mav, D., Shah, R.R., Shi, H., and Wade, P.A. (2013). MBD3 localizes at promoters, gene bodies and enhancers of active genes. PLoS Genet. *9*, e1004028.

Signolet, J., and Hendrich, B. (2015). The function of chromatin modifiers in lineage commitment and cell fate specification. FEBS J. *282*, 1692–1702.

Sousa-Victor, P., Gutarra, S., Garcia-Prat, L., Rodriguez-Ubreva, J., Ortet, L., Ruiz-Bonilla, V., Jardi, M., Ballestar, E., Gonzalez, S., Serrano, A.L., et al. (2014). Geriatric muscle stem cells switch reversible quiescence into senescence. Nature *506*, 316–321.

Stanley, E.G., Biben, C., Elefanty, A., Barnett, L., Koentgen, F., Robb, L., and Harvey, R.P. (2002). Efficient Cre-mediated deletion in cardiac progenitor cells conferred by a 3'UTR-ires-Cre allele of the homeobox gene Nkx2-5. Int. J. Dev. Biol. *46*, 431–439.

Vives-Bauza, C., Yang, L., and Manfredi, G. (2007). Assay of mitochondrial ATP synthesis in animal cells and tissues. Methods Cell Biol. *80*, 155–171.

Wenz, T., Diaz, F., Spiegelman, B.M., and Moraes, C.T. (2008). Activation of the PPAR/PGC-1alpha pathway prevents a bioenergetic deficit and effectively improves a mitochondrial myopathy phenotype. Cell Metab. *8*, 249–256.

Williams, C.J., Naito, T., Arco, P.G., Seavitt, J.R., Cashman, S.M., De Souza, B., Qi, X., Keables, P., Von Andrian, U.H., and Georgopoulos, K. (2004). The chromatin remodeler Mi-2beta is required for CD4 expression and T cell development. Immunity *20*, 719–733.

Yoshida, T., Hazan, I., Zhang, J., Ng, S.Y., Naito, T., Snippert, H.J., Heller, E.J., Qi, X., Lawton, L.N., Williams, C.J., and Georgopoulos, K. (2008). The role of the chromatin remodeler Mi-2beta in hematopoietic stem cell self-renewal and multilineage differentiation. Genes Dev. *22*, 1174–1189.

Zhang, J., Jackson, A.F., Naito, T., Dose, M., Seavitt, J., Liu, F., Heller, E.J., Kashiwagi, M., Yoshida, T., Gounari, F., et al. (2012). Harnessing of the nucleosome-remodeling-deacetylase complex controls lymphocyte development and prevents leukemogenesis. Nat. Immunol. *13*, 86–94.